

THERMONUCLEAR BURNING ON RAPIDLY ACCRETING NEUTRON STARS

LARS BILDSTEN

*Department of Physics and Department of Astronomy
366 LeConte Hall, University of California, Berkeley
Berkeley, CA 94720*

Neutron stars in mass-transferring binaries are accreting the hydrogen and helium rich matter from the surfaces of their companions. This article explains the physics associated with how that material eventually fuses to form heavier nuclei and the observations of the time dependent phenomena (such as Type I X-ray bursts) associated with the thermally unstable thermonuclear reactions. The majority of the article is pedagogical. Rather than just report from the computer output, we will (when possible) explain why things happen the way they do. This approach invariably comes at the expense of numerical accuracy but has the distinct advantage of explaining how the outcome depends on the composition of the accreting matter, the accretion rate and the mass, radius and thermal state of the neutron star. We also introduce many new analytic relations that are convenient for comparisons to both observations and computational results.

After explaining nuclear burning for spherically symmetric accretion onto neutron stars, we discuss the possibility of asymmetric burning. In particular, we discuss some of the mysteries from *EXOSAT* observations of Type I X-Ray bursts and how the solution to these puzzles may lie in considering the lateral propagation of nuclear burning fronts around the star. Fully understanding this problem requires knowledge of parameters previously neglected such as the distribution of fresh fuel on the star, the magnetic field strength, and the stellar rotation. Recent *RXTE* observations of bursters may finally tell us some of these parameters.

1. Introduction

Matter accreted onto a neutron star of mass M and radius R releases $GMm_p/R \approx 200$ MeV per nucleon, a value much larger than that released from thermonuclear fusion (7 MeV per nucleon for fusing hydrogen

to helium). Our lack of precise knowledge of the global accretion rate (\dot{M}) and M/R means that the luminosity from steady-state nuclear burning (i.e. at the same rate as it is accreted, $L_n = E_{nuc}\dot{M}$, where E_{nuc} is the nuclear energy released per gram) is impossible to distinguish from the accretion luminosity. Time dependent nuclear burning is more easily observed and is identified by having a time-averaged luminosity L_n .

Hansen & Van Horn (1975) first calculated how the accreted matter fuses to heavier elements in steady-state, and showed that almost all models were subject to the “thin-shell” thermal instability of Schwarzschild & Härm (1965). Though they did not investigate the time dependence of the unstable nuclear burning, Hansen and Van Horn concluded by noting:

“The wide range of time scales found – ranging from milliseconds to months, depending upon the stellar model – suggests the importance of a continued search for periodic or quasi-periodic phenomena over a similar range of time scales in the compact X-ray sources”

Such phenomena were soon found with the discovery of recurrent, quasi-periodic, Type I X-ray bursts from low accretion rate ($\dot{M} \lesssim 10^{-9} M_\odot \text{ yr}^{-1}$) neutron stars (Grindlay et al. 1976, Belian, Conner & Evans 1976). The successful association (Woosley & Taam 1976, Maraschi & Cavaliere 1977, Joss 1977, Lamb & Lamb 1978) of the thermal instabilities found by Hansen & Van Horn (1975) with the X-ray bursts made a nice picture of a recurrent cycle that consists of fuel accumulation for several hours followed by a thermonuclear runaway that burns the fuel in $\lesssim 10$ seconds. The observational quantity α (defined as the ratio of the time-averaged accretion luminosity to the time-averaged burst luminosity) was of the order the expected value (i.e. $\alpha = (GM/R)/E_{nuc} \approx 15 - 30$) for a thermonuclear origin of the bursts. This has proven to be one important test for attributing any time-dependent phenomenon to nuclear burning. As we discuss here, the nature of the time dependence need not always be the simple limit-cycle behavior of Type I X-ray bursts.

We are focused solely on neutron stars accreting globally at rates in excess of $10^{-10} M_\odot \text{ yr}^{-1}$, which is appropriate for most bright, persistent Low Mass X-ray binaries (in particular the “Z” and “Atoll” sources of Hasinger & van der Klis 1989). We begin in §2 by explaining the physics of steady-state nuclear burning and discussing the “thin-shell” thermal instability. Section 3 is a derivation of the ignition conditions and an explanation of the accretion rate dependent regimes of unstable burning. The energetics, recurrence times and durations of the bursts are discussed in §4. We do not review much of the pre-RXTE observations of Type I X-Ray bursts, as there are many reviews for that material (see Lewin, van Paradijs and Taam, 1995 for the most recent summary of observations of Type I X-ray bursts, including details of radius expansion bursts which are not discussed

here). However, we do summarize (in §4.2) what was learned from *EXOSAT* observations of bursters, as these pointed to the possibility of asymmetric burning.

Section 5 opens up the discussion of asymmetric burning and presents what is known about the speed of propagation of burning fronts on neutron stars. It is often said that “X-ray Pulsars Don’t Burst” and “X-ray Bursters don’t Pulse”. Section 6 discusses this dichotomy in some detail and points out those accreting pulsars which might someday violate this “rule”, especially the recently discovered pulsar GRO J1744-28 (Kouveliotou et al. 1996, Finger et al. 1996). We close in §7 by summarizing the recent RXTE results on coherent oscillations during Type I X-ray bursts.

2. Thermal Stability of Steady State Nuclear Burning

Most neutron stars are accreting a mix of hydrogen and helium from a relatively unevolved companion star. The standard case we consider here has a hydrogen mass fraction of $X = 0.7$. In this case, most of the nuclear energy release is from fusion of the hydrogen to helium. The very high temperatures reached ($T \gtrsim 10^9$ K) when this burning is unstable leads to production of elements near the iron group. In the steady-state burning case, the temperatures in the hydrogen/helium burning region are not as high and so the fusion to the iron group elements occurs at much larger depths. It is also important to keep in mind that the CNO metallicity (Z_{CNO}) of the accreting material can vary by a few orders of magnitude, depending on what stellar population the companion is from.

2.1. EQUATIONS AND DEFINITIONS

Most workers use the global accretion rate, \dot{M} , as the fundamental parameter for discussion of the state of nuclear burning. However, the plane-parallel nature of the neutron star atmosphere means that the physics of thermal stability and nuclear ignition actually depends on the accretion rate per unit area, \dot{m} (Fujimoto, Hanawa & Miyaji 1981, hereafter FHM). This parameter determines the local behavior on the neutron star and need not be the same everywhere. The local Eddington rate is

$$\dot{m}_{\text{Edd}} = \frac{2m_p c}{(1+X)R\sigma_{\text{Th}}} = \frac{1.5 \times 10^5 \text{ g cm}^{-2} \text{ s}^{-1}}{(1+X)} \left(\frac{10 \text{ km}}{R} \right), \quad (1)$$

where σ_{Th} is the Thomson scattering cross-section, m_p is the proton mass and c is the speed of light. The ram pressure within the accreted and settling atmosphere is negligible, so that hydrostatic balance yields $P = gy$, where $dy = -\rho dz$ is the column depth (in units of g cm^{-2}) and $g \approx GM/R^2$ (we

neglect general relativistic corrections throughout this article). The local pressure scale height, $h = P/\rho g$, is always $\ll R$ and so g is nearly constant and the atmosphere is geometrically thin. The flux is carried by radiative transport and, for the accretion rates of interest here, the main atmospheric opacity is Thomson scattering, $\kappa = \kappa_{es} = \sigma_{\text{Th}}(1+X)/2m_p$. The flux leaving the plane parallel atmosphere is then

$$F = -\frac{c}{3\kappa\rho} \frac{d}{dz} aT^4 = \frac{c}{3\kappa} \frac{d}{dy} aT^4, \quad (2)$$

where a is the radiation constant. For a constant flux, this integrates to

$$T^4 = \frac{3\kappa P F}{acg}, \quad (3)$$

at pressures large relative to the photospheric value $P_{ph} \approx g/\kappa$ (i.e. the radiative zero solution, Schwarzschild 1958).

Steady accretion modifies the equations of particle continuity and entropy for hydrostatic settling of the atmosphere (FHM). One rewrites these equations in a coordinate system of fixed pressure. In this case the accreted matter flows through the coordinates as it is compressed by accretion of fresh material from above. The continuity equation for an element i (with number density n_i) is

$$\frac{\partial n_i}{\partial t} + \vec{\nabla} \cdot (n_i \vec{v}) = \sum r, \quad (4)$$

where r is the sum of particle creation and destruction processes. For high accretion rates, there is not time for differential settling (i.e. diffusion of one charged species relative to another) and all elements co-move downward at the speed needed to satisfy mass continuity, $v = \dot{m}/\rho$ (Wallace, Woosley & Weaver 1982, Bildsten, Salpeter & Wasserman 1993). We then define a mass fraction $X_i \equiv \rho_i/\rho = A_i m_p n_i/\rho$ where A_i is the baryon number of species i and expand the continuity equation to obtain

$$\frac{\partial X_i}{\partial t} + \dot{m} \frac{\partial X_i}{\partial y} = \frac{A_i m_p \sum r}{\rho}. \quad (5)$$

The equation for the entropy is

$$T \frac{ds}{dt} = -\frac{1}{\rho} \vec{\nabla} \cdot \vec{F} + \epsilon, \quad (6)$$

where ϵ is the energy release rate from nuclear burning. We write the entropy as $T ds = C_p T (dT/T - \nabla_{\text{ad}} dP/P)$, where $\nabla_{\text{ad}} = d \ln T / d \ln P$ for an

adiabatic change and C_p is the specific heat at constant pressure. Then since the temperature can depend on both time and pressure, we find

$$\frac{\partial F}{\partial y} + \epsilon = C_p \left(\frac{\partial T}{\partial t} + \dot{m} \frac{\partial T}{\partial y} \right) - \frac{C_p T \dot{m}}{y} \nabla_{\text{ad}}. \quad (7)$$

These are the equations that describe the hydrostatic evolution of the neutron star atmosphere and are valid while the matter accumulates on the neutron star. The thermonuclear instability can sometimes lead to outflow and hydrodynamics, for which these equations cannot be used.

2.2. THE UPPER ATMOSPHERE BEFORE BURNING

The neutron stars in low-mass X-ray binaries accrete via an accretion disk formed in the Roche lobe overflow of the stellar companion. There are still debates about the “final plunge” onto the neutron star surface, with some advocating that there is a strong enough magnetic field to control the final infall, while others prefer an accretion disk boundary layer. The only known effect on the later nuclear burning is that substantial destruction of all elements heavier than helium via spallation reactions can occur if the final plunge has an appreciable radial component (Bildsten, Salpeter & Wasserman 1992). The predicted amounts of spallation are substantial and basically turn the accreted matter into hydrogen, helium and a mix of light fragments, none of them capable of sustaining a CNO cycle.

Eventually the accreted material reaches the stellar surface, thermalizes and radiates away nearly all of the ≈ 200 MeV nucleon $^{-1}$ infall energy. Hence, the flux exiting the star a few scale heights beneath the thermalizing region is from energy released much deeper within the star, due to gravitational settling and nuclear burning. At this point, the matter is part of the star and is in hydrostatic balance. It is continuously compressed by the accretion of new material from above and eventually reaches pressures and temperatures adequate for thermonuclear ignition. The equations describing the settling and compression of the the atmosphere are heat transfer (equation [2]) and entropy (equation [7]). Rather than give a detailed discussion of these “settling” solutions, let’s just compare terms in the entropy equation in order to show what is most important.

The compression occurs on a timescale $t_{\text{accr}} \approx y/\dot{m}$, which we compare to the thermal timescale set by radiative diffusion

$$t_{\text{th}} \approx \frac{3\kappa C_p y^2}{4acT^3}, \quad (8)$$

in order to discover whether the compression is adiabatic. Presuming that the atmosphere at some column depth y is carrying a flux, F , then the ratio

of these two timescales is

$$\frac{t_{th}}{t_{accr}} \sim \frac{C_p T \dot{m}}{F}, \quad (9)$$

so that, when $F \gg C_p T \dot{m} \approx 5k_B T \dot{m} / 2\mu m_p$ the thermal time is much less than the rate of compression, where μ is the mean molecular weight of the accreting gas. This is always the case in the upper atmosphere ($\rho < 10^6 \text{ g cm}^{-3}$), as the energy released per proton from either steady burning or deeper gravitational settling is much more than $k_B T$ in the upper atmosphere. In this regime, the ‘‘trajectory’’ of the compressed fluid element is far from adiabatic as it has time to transport heat while it is being compressed. This simplifies the calculation, as the temperature gradient in the upper atmosphere is then set by the flux. The outer boundary condition plays no role.¹ These settling solutions are valid until the helium burns fast enough to appreciably change either the temperature or the helium abundance.

For the high accretion rates of interest here, most of the outer envelope is non-degenerate so $P = \rho k_B T / \mu m_p = gy$. We can always correct the equation of state for degeneracy by reducing μ to $\mu_{eff} = \rho k_B T / P m_p < \mu$. The temperature profile is determined by the flux flowing through the atmosphere, which is presumed to be a constant $F = E_{atm} \dot{m}$, where E_{atm} is the energy released per accreted gram at some large depth in the atmosphere. This parameter will be determined later and depends on whether the burning is in steady-state or not. Then when the flux is written as $F = 10^{23} E_{18} \dot{m}_5 \text{ ergs cm}^{-2} \text{ s}^{-1}$, where $E_{atm} = E_{18} 10^{18} \text{ ergs g}^{-1}$ and $\dot{m} = \dot{m}_5 10^5 \text{ g cm}^{-2} \text{ s}^{-1}$, the relation between the density and temperature in the upper atmosphere from equation (3) is

$$T_8 = 3.32 \rho_5^{1/3} \left(\frac{E_{18} \dot{m}_5 (1 + X) 0.6}{g_{14} \mu} \right)^{1/3} \quad (10)$$

where $T = T_8 10^8 \text{ K}$, $\rho = \rho_5 10^5 \text{ g cm}^{-3}$ and $g = g_{14} 10^{14} \text{ cm s}^{-2}$.² This gives a good first cut at how the temperature changes with depth in the accreting envelope above the burning region.

As mentioned earlier, the short thermal time leads to an entropy loss for the compressing fluid elements. Using the above relation, we find that $s \propto \ln(T^{3/2}/\rho) \propto \ln(1/\rho^{1/2})$, and so it is clear that the entropy of the

¹The problem is much more subtle when the thermal time at some depth is comparable to the local compression time, y/\dot{m} . For neutron stars, this is only known to happen at accretion rates far in excess of the Eddington rate at depths beneath the hydrogen and helium burning (Bildsten & Cutler 1995, Brown & Bildsten 1997).

²I use \dot{m}_5 as the local unit for the accretion rate, which is related to the global supply onto the neutron star via $\dot{M} = \dot{m}_5 2 \times 10^{-8} M_\odot \text{ yr}^{-1} (R/10 \text{ km})^2$.

accreting material actually decreases as it is compressed to higher densities. This temperature profile is convectively stable and will allow us to find where the nuclear burning begins. The convectively stable atmosphere has internal buoyancy that is measured by the Brunt-Väisälä frequency (Cox 1980)

$$N^2 = -g \left(\frac{d \ln \rho}{dz} - \frac{1}{\Gamma_1} \frac{d \ln P}{dz} \right) = -g \left(\frac{d \ln \rho}{dz} + \frac{1}{\Gamma_1 h} \right), \quad (11)$$

where $h = P/\rho g \ll R$ is the local scale height and $\Gamma_1 = (d \ln P/d \ln \rho)_{adiab} = 5/3$ is the adiabatic index. The temperature-density profile for a constant flux atmosphere then gives

$$N^2 = \frac{3g}{20h} = \frac{3\mu m_p g^2}{20k_B T}, \quad (12)$$

which decreases with depth in the star since the temperature rises. The frequency of local buoyant oscillations is then $N \approx (50 \text{ kHz}) g_{14}/T_8^{1/2}$, comparable to the inverse of the time it takes sound to travel a scale height.

2.3. HOW HYDROGEN BURNS AT HIGH ACCRETION RATES

For these high accretion rates, the atmospheric temperature is always in excess of 10^7 K, so that hydrogen burns via the CNO cycle. However, at large densities and high temperatures, the timescale for proton captures becomes shorter than the subsequent β decay lifetimes.

For example, consider the $^{14}\text{N}(p,\gamma)^{15}\text{O}$ reaction, which is one of the slower steps in the cycle. The timescale for the proton capture is $t_{cap} = (n_p \langle \sigma v \rangle)^{-1}$, where $\langle \sigma v \rangle$ is the thermally averaged reaction rate from Caughlan & Fowler (1988), and becomes shorter than a typical β decay time of 100 seconds when $T > 8 \times 10^7$ K for the relevant density of $\rho = 10^5 \text{ g cm}^{-3}$. These temperatures are usually reached before the unstable ignition of helium takes place. The rapid proton captures makes a slightly different burning cycle than typically encountered, which is called the hot CNO cycle (Hoyle & Fowler 1965)



The time to go around this catalytic hydrogen burning loop is set by the β decay lifetimes of ^{14}O ($t_{1/2} = 71 \text{ s}$) and ^{15}O ($t_{1/2} = 122 \text{ s}$) and is *temperature independent* and thermally stable. While this cycle is operative, all of the seed nuclei are locked up in ^{14}O and ^{15}O . These β -decay limitations fix the hydrogen burning rate at

$$\epsilon_h = 5.8 \times 10^{15} Z_{\text{CNO}} \text{ ergs g}^{-1} \text{ s}^{-1}, \quad (14)$$

where Z_{CNO} is the mass fraction of CNO in the accumulating matter.

There is thus a minimum column density of fresh fuel needed on the star, y_h , to burn the hydrogen at the rate at which it is accreted (i.e. steady-state). It is found by setting $\epsilon_h y_h = \dot{m} X E_h$ where $E_h \approx 6.4 \times 10^{18}$ ergs g^{-1} is the energy released from hydrogen burning to helium, giving

$$y_h \approx 10^{10} \text{ g cm}^{-2} X \dot{m}_5 \left(\frac{0.01}{Z_{\text{CNO}}} \right). \quad (15)$$

This is equivalent to the amount of matter accreted onto the star in the time it takes to go around the cycle enough times to consume all of the hydrogen, $E_h/\epsilon_h \approx (10^3/Z_{\text{CNO}})\text{s}$, or about one day for typical metallicities. However, the matter will reach high enough temperatures within a day of landing on the neutron star so that the primordial helium can ignite. In this case helium burning occurs in a hydrogen-rich environment, which enhances the nuclear reaction chains and energy release (Lamb & Lamb 1978; Taam & Picklum 1978, 1979; FHM; Taam 1982).

2.4. WHEN DOES THE HELIUM START BURNING?

Now let's ask when the helium ignites and whether or not it is thermally stable. The energy generation rate for helium burning to carbon is (Hansen & Kawaler 1994)

$$\epsilon_{3\alpha} = 5.3 \times 10^{21} \frac{\rho_5^2 Y^3}{T_8^3} \exp\left(\frac{-44}{T_8}\right) \text{ ergs g}^{-1} \text{ s}^{-1}. \quad (16)$$

In a steady-state burning situation, the helium depletes at the depth where the lifetime to the nuclear reaction equals the time it takes to cross a scale height (Taam 1981, Fushiki & Lamb 1987)

$$\frac{\dot{m} Y}{y} \approx \frac{\epsilon_{3\alpha}}{E_{3\alpha}}, \quad (17)$$

where $E_{3\alpha} = 5.84 \times 10^{17}$ ergs g^{-1} is the energy release from $3\alpha \rightarrow {}^{12}\text{C}$. Even when hydrogen is present, this condition is the appropriate one, as the carbon produced from helium burning increases the number of seed nuclei for the hot CNO cycle and allows for more rapid hydrogen consumption.

The helium depletion condition (equation [17]) is now combined with the temperature profile (see equation [10]; we leave the energy released per accreted particle, E_{18} , as a free parameter) to find the temperature at which the helium is burned

$$\dot{m}_5^4 = 68.2 \left[\frac{(Y g_{14} \mu)^2 T_8^7}{(1+X)^3 E_{18}^3} \right] \exp\left(\frac{-44}{T_8}\right). \quad (18)$$

Solving this transcendental equation for the temperature also gives the pressure for the helium burning, and most importantly, how these quantities depend on the local accretion rate, stellar mass and radius, and abundances. In order to simplify the transcendental, expand the exponential about the temperature of $T_8 = 3.38$ so that $\exp(-44/T_8) \approx 2.22 \times 10^{-6} (T_8/3.38)^{13}$. Some accuracy is compromised because of this approximation, but not much. The resulting equation for the burning temperature is

$$\begin{aligned} T_{burn} &= 3.43 \times 10^8 \text{K} \dot{m}_5^{1/5} \frac{(E_{18} + X E_{18})^{3/20}}{(Y g_{14} \mu)^{1/10}}, \\ &= \text{Temperature at Helium Burning Location.} \end{aligned} \quad (19)$$

The very strong temperature sensitivity of the helium burning makes this temperature estimate fairly accurate. The column density at the burning location is

$$y_{burn} = \frac{5.2 \times 10^7 \text{ g cm}^{-2}}{\dot{m}_5^{1/5} (E_{18} Y g_{14} \mu (1 + X))^{2/5}}, \quad (20)$$

which is a bit trickier to compare to a real calculation that finds the abundance profiles self-consistently.

For example, a full integration from Bildsten & Brown (1997) for a star with $g_{14} = 1.87$, $X = 0.7$, and $Y = 0.3$ accreting at $\dot{m}_5 = 1$ and burning in steady-state (so that $E_{18} = 5.3$) found that one-half of the accreted helium is burned at a location where $T_8 = 5.38$, $y = 8.3 \times 10^7 \text{ g cm}^{-2}$ and $\rho = 2 \times 10^5 \text{ g cm}^{-3}$. The matter is non-degenerate and the opacity is slightly less than Thomson scattering $\kappa \approx 0.4 \kappa_{es} \approx 0.136 \text{ cm}^2 \text{ g}^{-1}$. Our formulae (equations [19] and [20]) give $T_8 = 5.32$ and $y_{burn} = 3.3 \times 10^7 \text{ g cm}^{-2}$ for this case. As you can see the temperature is in excellent agreement. Even when we correct for the lower opacity, the estimated column is nearly a factor of 2 low relative to the numerical estimate. This is because we have found the place where the lifetime of an alpha particle is comparable to the time since arrival on the star. To completely burn the matter in steady-state requires a time longer than this and is roughly $t_{burn} \approx 10^3 \text{ s} / \dot{m}_5^{6/5}$ or < hour at accretion rates where the burning is stable.

We can now check the previous statement that the helium ignites before the hydrogen has completely burned. This is true for high accretion rates, as $y_{burn} < y_h$ (compare equations [15] and [20]) as long as $\dot{m}_5 > 0.016 (0.01/Z_{CNO})^{5/6}$. All steady-state solutions that we find at high accretion rates are burning the helium in a hydrogen-rich environment.

2.5. THERMAL STABILITY OF STEADY-STATE HELIUM BURNING

Let's now understand whether these models are stable to a thermal perturbation. It is best to start by writing down the energy equation. Since we

are considering a thermal perturbation on a timescale much shorter than the time it takes for the matter to move a scale height, all terms $\propto \dot{m}$ in equation (7) can be dropped, giving

$$C_p \frac{\partial T}{\partial t} = \frac{\partial F}{\partial y} + \epsilon. \quad (21)$$

It is a good approximation to presume a constant pressure during the thermal perturbations. The simplest linear stability analysis of the steady-state model presumes just one zone (i.e. single pressure, Fujimoto et al. 1981) and so we set

$$\frac{\partial F}{\partial y} \approx -\frac{acT^4}{3\kappa y^2} \equiv \epsilon_{cool}, \quad (22)$$

as the simple representation of the radiative cooling rate from the atmosphere. The β -limited hydrogen burning is temperature independent, so that the instability must arise from helium ignition. Writing $\epsilon_{3\alpha} \propto T^\nu \rho^\eta$, where $\nu = 44/T_8 - 3$, a constant pressure perturbation of the equilibrium model (i.e. $\epsilon = -\epsilon_{cool}$) is stable when

$$\nu - 4 + \frac{d\ln\kappa}{d\ln T} + \frac{d\ln\rho}{d\ln T} \left(\eta + \frac{d\ln\kappa}{d\ln\rho} \right) < 0, \quad (23)$$

where all the derivatives are at constant pressure. These steady-state solutions are only marginally degenerate (the density at a given pressure and temperature never differs from the non-degenerate guess by more than 15%) in the burning region and so $d\ln\rho/d\ln T = -1$. In addition, the opacity is not far from Thomson scattering, so those derivatives are zero, making the condition just $\nu < 4 + \eta$ for stability, clearly displaying that the thermal stability is a competition between nuclear heating and radiative cooling (which scales $\propto T^4$). We thus need $T > 4.88 \times 10^8$ K for stable helium burning. More sophisticated non-local linear analysis have been carried out by Fushiki & Lamb (1987).

For a thin shell, the degree of degeneracy has only a small effect on the stability criterion and, most importantly, this instability does not require that the matter be degenerate. The more important condition is that it is thin ($h \ll R$) so that its temperature increases when it is heated (i.e. a positive specific heat, $C_p > 0$). It is clearly thin before burning and remains so even during the flash as the large gravitational well on the neutron star requires temperatures of order 10^{12} K for $h \sim R$. Temperatures this high are never reached. This analysis provides a reasonable indicator of when we should expect time dependence of the burning. The strength of the “flashes” is sensitive to the non-linearity of the nuclear reaction rates, such as the weakening of the temperature dependence at higher temperatures, and the decreasing density as the temperature rises at fixed pressure.

We are lucky that it is temperature which determines stability, as this is the quantity that is best determined by this analytic calculation. The above discussion basically pointed to the condition $T_{burn} > 4.88 \times 10^8 \text{K}$ for stability, which, from equation (19) turns into a condition

$$\dot{m} > \dot{m}_{st} = 5.83 \times 10^5 \frac{\text{g}}{\text{cm}^2 \text{ s}} \frac{(Y g_{14} \mu)^{1/2}}{[(1+X)E_{18}]^{3/4}} \left(\frac{\kappa_{es}}{\kappa} \right)^{3/4} \quad (24)$$

for stable helium ignition. We first evaluate this for accretion of pure helium and then discuss in more detail the more prevalent case of accretion of hydrogen-rich material. In both instances, we will define an accretion rate, \dot{m}_{st} , above which the helium burning is thermally stable.

There are a few ultra-compact ($P_{orb} < 50 \text{ min}$) binaries (4U 1820-30, 4U 1916-05 and 4U 1626-67, Nelson, Rappaport & Joss 1986) which are most likely accreting pure helium from a degenerate dwarf. The smaller nuclear energy released per gram for helium accretion (relative to hydrogen-rich accretion) means that the flux flowing through a steady-state burning envelope is less (Joss 1978, Joss & Li 1980, Bildsten 1995). Let's consider the steady-state helium burning case, where $Y = 1$, $X = 0$, $\mu = 4/3$ and $E_{18} = 0.58$, in which case the accretion rate needed for stability is

$$\dot{m}_{st}(\text{Pure Helium}) \approx 1.4 \times 10^6 \frac{\text{g}}{\text{cm}^2 \text{ s}} \left(\frac{M}{1.4M_{\odot}} \right)^{1/2} \left(\frac{10 \text{ km}}{R} \right), \quad (25)$$

20 times higher than the hydrogen-rich limit we will discuss next. This is due to the reduced amount of energy release from helium burning and allows for the bright helium accreting object 4U 1820-30 (see Bildsten 1995 for a detailed discussion) to be violently unstable at accretion rates $\sim 10^{-8} M_{\odot} \text{ yr}^{-1}$.

2.6. STABLE HYDROGEN AND HELIUM BURNING

Most neutron stars are accreting from relatively unevolved companions and so $X = 0.7$, $Y = 0.3$ and $\mu = 0.6$. The energy released when steadily burning all the hydrogen and helium to, say, carbon is $E_{18} = 5.3$. This gives a critical local accretion rate for stable helium burning in this mixed environment of

$$\dot{m}_{st}(\text{H/He}) \approx 6.5 \times 10^4 \frac{\text{g}}{\text{cm}^2 \text{ s}} \left(\frac{M}{1.4M_{\odot}} \right)^{1/2} \left(\frac{10 \text{ km}}{R} \right) \left(\frac{\kappa_{es}}{\kappa} \right)^{3/4}. \quad (26)$$

We can also write this in terms of the global Eddington rate

$$\frac{\dot{M}_{st}}{\dot{M}_{Edd}} \approx 1.5 \left(\frac{Y}{0.3} \frac{\mu}{0.6} \frac{M}{1.4M_{\odot}} \right)^{1/2} \left(\frac{1+X}{1.7} \right)^{1/4} \left(\frac{0.4\kappa_{es}}{\kappa} \right)^{3/4}, \quad (27)$$

where we have inserted the typical ratio of the opacities in the burning region. There is no reason to believe that this calculation is accurate enough to say whether the critical accretion rate for burning is above or below the Eddington rate. What is more trustworthy are the scalings, and notice that equation (27) is independent of the stellar radius and weakly dependent on the stellar mass. Using the estimate of the critical accretion rate (equation [27]), one finds that neutron stars brighter than $L_{accr} = GMM_{st}/R \approx 2 \times 10^{38} (M/1.4M_{\odot})^{3/2}$ ergs s⁻¹ should be stably burning the hydrogen and helium. Note that a more massive neutron star can have unstable nuclear burning at higher accretion luminosities than a less massive star. This might provide a possible indicator of mass for those objects where the distance is reasonably well known.

Fujimoto et al. (1981) estimated \dot{M}_{st} (they called it \dot{M}_{cri} in their Table 1) for 3 different neutron stars. They found $\dot{M}_{st}/(10^{-9}M_{\odot} \text{ yr}^{-1}) = 15, 13,$ and 12 for $M = 0.476, 1$ and $1.41M_{\odot}$. Our numbers inferred from equation (26) are $\dot{M}_{st}/(10^{-9}M_{\odot} \text{ yr}^{-1}) = 13, 16,$ and 17 for the same three masses and radii. These are about 20 – 30% different. The most accurate way to learn if the burning is thermally stable is to numerically solve the time dependent equations (3), (5) and (7). Ayasli & Joss (1982) and Taam, Woosley & Lamb (1996) performed time-dependent calculations at accretion rates comparable to the Eddington limit and found that the burning is still thermally unstable when $\dot{M} \lesssim \dot{M}_{Edd}$. Ayasli & Joss (1982) also carried out a few super-Eddington (by a few) calculations and found thermal stability, in agreement with the calculations here. However, there has not been a thorough study (i.e. surveying the dependence of \dot{M}_{st} on M, R and composition) of this problem. Indeed, little has been published on the steady-state burning of matter on accreting neutron stars at super-Eddington accretion rates. The most likely environment for this burning is on the polar caps of high accretion rate pulsars (see §6).

3. Unstable Mixed Hydrogen/Helium Burning

Since most neutron stars in LMXB's are less luminous than 10^{38} ergs s⁻¹, we should expect some sort of time-variable phenomena from nuclear burning. We will find that, in one dimension, the system evolves into a limit cycle, accumulating fuel for some long time and then reaching a thermal instability which leads to observable phenomena.

3.1. THERMONUCLEAR IGNITION CONDITIONS

How much matter needs to be accreted before reaching an instability? In order to keep things simple, let's presume that the accreted matter has a metallicity large enough so that the flux leaving the accreting envelope

is just $F = \epsilon_h y_t$ prior to reaching an instability, where y_t is the column of freshly accreted matter on the star since the last thermal instability (Taam 1980, Wallace, Woosley & Weaver 1982).³ The condition for the thermal instability is slightly different for these non-equilibrium solutions, since the entropy equation before the instability is balancing heat diffusion with the energy released from the hot CNO cycle and gravitational settling. However, neither of these energy sources can lead to a thermal instability. It is the helium burning which takes care of that.

The boundary of unstable/stable helium burning in the $y - T$ plane is defined by the relation

$$\frac{d\epsilon_{3\alpha}}{dT} = -\frac{d\epsilon_{cool}}{dT}, \quad (28)$$

(FHM, Hanawa & Fujimoto 1982, Fushiki & Lamb 1987), where ϵ_{cool} is defined by equation (22). These derivatives are taken at constant pressure, as the instability grows faster than the pressure changes. Let's presume some knowledge about the answer and expand the exponential in the helium burning rate at $T_8 = 2.31$ so that we get a simple relation for the ignition temperature on the unstable branch of the relation (equation [28])

$$T_{\text{ign}} \approx \frac{1.83 \times 10^8 \text{K}}{\kappa^{1/10} Y^{3/10} (\mu g_{14} y_8^2)^{1/5}}. \quad (29)$$

The freshly accreted matter is then linearly unstable to a thermal perturbation when $T > T_{\text{ign}}$ at the specified column density. This is a linear instability and needs no “trigger”. It is just that (on the unstable branch) any slight upward temperature perturbation will lead to more rapid nuclear energy release than cooling. There is a stable branch for the ignition condition at higher temperatures (see heavy dashed line in Figure 1), where a positive temperature perturbation leads to more rapid cooling. The dark solid and dashed line in Figure 1 displays the complete ignition relation (equation [28]) for a neutron star of mass $1.4M_\odot$ and $R = 10$ km accreting matter with $Y = 0.3$.

Thermally unstable ignition of the accreting matter will occur if the settling matter reaches the unstable part of the ignition curve (dark solid) before burning all of the helium. Now, what is the temperature at the bottom of the accumulating matter? The flux in the atmosphere prior to the unstable helium ignition is just that generated from the stable hydrogen burning, $F(y) = \epsilon_h(y_t - y)$, which when combined with the radiative transfer

³This requires that $\epsilon_h y_t \gtrsim k_B T / m_p \dot{m}$ so that we can neglect the energy release from the compression of matter or just $Z_{CNO} \gtrsim 10^{-3} T_8 \dot{m}_5 / y_8$. As we discuss in §3.3, this condition will be violated for interesting values of the metallicity, in which case the ignition conditions depend on the accretion rate, \dot{m} .

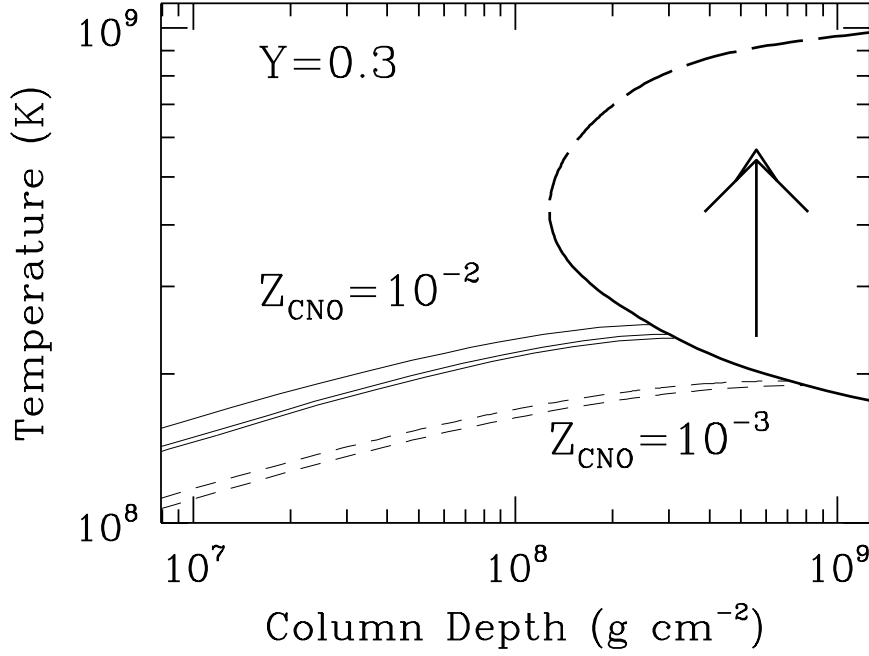


Figure 1. Ignition conditions on an accreting neutron star of mass $M = 1.4M_{\odot}$ and $R = 10$ km. The thick solid curve is the unstable portion of helium ignition (equation [29]). The atmosphere is thermally unstable to the right of this line. The heavy dashed line is the stable branch. The three thin solid lines are settling solutions (from bottom to top) for $Z_{CNO} = 10^{-2}$ and $\dot{m}_5 = 0.3, 0.75$ and 3 . The two thin dashed lines are for $Z_{CNO} = 10^{-3}$ and $\dot{m}_5 = 0.15$ and 0.75 . The upward pointing arrow shows the direction in which the temperature evolves when the thermal instability occurs.

equation gives a relation

$$T^4 = \frac{3\kappa\epsilon_h y_t^2}{2ac}. \quad (30)$$

It is the intersection of this solution with the ignition condition (equation [29]) that tells us the temperature

$$T_{\text{ign}} \approx 3.5 \times 10^8 \text{K} \frac{\kappa^{1/18}}{Y^{1/6}} \left(\frac{Z_{CNO}}{\mu g_{14}} \right)^{1/9}, \quad (31)$$

and column density

$$y_{\text{ign}} \approx \frac{2 \times 10^7 \text{ g cm}^{-2}}{Y^{1/3} \kappa^{7/18} Z_{CNO}^{5/18}} \left(\frac{1}{\mu g_{14}} \right)^{2/9}, \quad (32)$$

for the unstable ignition of helium in the hydrogen-rich environment. Both of these parameters are relatively insensitive to the value of the opacity. It

is important to point out that the ignition pressure, $P = gy_{ign} \propto g^{7/9}$ and therefore the outcome of the unstable helium flash depends on the neutron star mass and radius. This is in contrast to thermonuclear instabilities on accreting white dwarfs, where the ignition pressure is nearly independent of gravity, thus allowing for simple relations between the recurrence time and accretion rate (Shore, Livio and van den Heuvel 1994).

The electrons are mildly degenerate at the ignition site, where the typical density is $\rho \sim (5 - 8) \times 10^5 \text{g cm}^{-3}$. Putting in characteristic values for these quantities, namely $Y = 0.3$ and $\mu = 0.6$ (we could correct for degeneracy to μ_{eff} , but the ignition column is not that sensitive to it), we find that the ignition conditions are

$$T_{ign} \approx 2.12 \times 10^8 \text{ K} \left(\frac{\kappa}{0.04 \text{ cm}^2 \text{ g}^{-1}} \right)^{1/18} \left(\frac{Z_{CNO}}{0.01} \right)^{1/9} \left(\frac{1.87}{g_{14}} \right)^{1/9}, \quad (33)$$

and

$$y_{ign} \approx 3.7 \times 10^8 \frac{\text{g}}{\text{cm}^2} \left(\frac{0.04 \text{ cm}^2 \text{ g}^{-1}}{\kappa} \right)^{7/18} \left(\frac{0.01}{Z_{CNO}} \right)^{5/18} \left(\frac{1.87}{g_{14}} \right)^{2/9}, \quad (34)$$

where we have scaled the opacity to the values found from calculations which include electron conduction. This formula compares well with that of Fujimoto et al. (1987), who found $y_{ign} \propto Z_{CNO}^{-0.5}$. These calculations also tell us that the physical thickness of the accumulated layer prior to the instability is 10 meters, an important point for later reference. After discussing the different accretion rate regimes for burning, we will come back and use these results for predicting the nature of the resulting Type I X-Ray bursts.

The three light solid lines are the envelope conditions just prior to unstable helium ignition for $Z_{CNO} = 10^{-2}$ and local accretion rates of $\dot{m}_5 = 0.3, 0.75,$ and 3 (Bildsten & Brown 1997). These solutions should be viewed as upper limits to the ignition column density, as they presume that there is no flux at the bottom ($y = y_t$) of the accumulating material. Note that, as derived above, the ignition conditions are nearly independent of the local accretion rate. The ignition conditions found numerically are $y_{ign} \approx 3 \times 10^8 \text{g cm}^{-2}$, $T_{ign} \approx 2.4 \times 10^8 \text{K}$ and $\rho \approx 8 \times 10^5 \text{g cm}^{-3}$, a factor of 0.45 less dense than we would have guessed if the electrons were non-degenerate (see equations [33] and [34]). In this case, degeneracy is starting to play a role. The flux exiting the atmosphere is larger than just $\epsilon_h y_{ign}$ due to the internal gravitational energy release.

We also show two settling solutions for a lower metallicity of $Z_{CNO} = 10^{-3}$ and $\dot{m}_5 = 0.15$ and 0.75 (the two dashed lines). For metallicities this low the ignition conditions become dependent on \dot{m} (see discussion in §3.3).

This is evident in Figure 1, where $y_{ign} \approx 7 \times 10^8 \text{ g cm}^{-2}$ for $\dot{m}_5 = 0.75$ and $y_{ign} \approx 8 \times 10^8 \text{ g cm}^{-2}$ for $\dot{m}_5 = 0.15$. Degeneracy is becoming more important ($\mu_{eff} \approx 0.3\mu$), thus changing the opacity to $\kappa \approx 0.01 \text{ cm}^2 \text{ g}^{-1}$. It is still the case though that our equations (34) and (33) can reasonably well represent what is found in the numerical simulations for the ignition.

3.2. THE ACCRETION RATE DEPENDENCE OF UNSTABLE BURNING

We now ask how the nature of the unstable burning depends on the local accretion rate. It ends up that there are two critical accretion rates that happen to overlap with the range of accretion rates relevant to the bright X-ray binaries.

At very high \dot{m} 's, the helium unstably ignites at the bottom of the freshly accumulated pile prior to hydrogen exhaustion, or $y_h > y_{ign}$ (Taam & Picklum 1978, 1979, Taam 1980). This translates into a critical accretion rate

$$\dot{m}_{c1} \approx \frac{4.2 \times 10^3 \text{ g cm}^{-2} \text{ s}^{-1}}{g_{14}^{2/9} X} \left(\frac{0.04 \text{ cm}^2 \text{ g}^{-1}}{\kappa} \right)^{7/18} \left(\frac{Z_{CNO}}{0.01} \right)^{13/18}, \quad (35)$$

so that when $\dot{m} > \dot{m}_{c1}$ the helium ignites in a hydrogen-rich environment. This formula agrees very well with the results of Hanawa & Fujimoto (1982) for $g_{14} < 2$, even the scaling with the surface gravity. It also reproduces the critical accretion rates in Taam (1981) to within a factor of two for a range in metallicities and neutron star masses and radii.⁴

For accretion rates below this value ($\dot{m} < \dot{m}_{c1}$), the hydrogen burns steadily and accumulates a pure helium shell underneath it. The column density of hydrogen on the star is just given by equation (15), and beneath this a pure helium shell accumulates with time until a thermal instability is eventually reached. The helium ignition is always unstable. We will not derive the necessary conditions for the helium flash, but rather find the accretion rate below which the hydrogen burning shell becomes thermally unstable. This will happen when the temperature in the hydrogen burning region becomes low enough (roughly $T < 8 \times 10^7 \text{ K}$, see §2.3) so that the proton capture reactions again determine the time to go around the CNO cycle loop. In this case, the temperature sensitivity of the CNO burning ($\nu \approx 11/T_8^{1/3}$ from the $^{14}\text{N}(p,\gamma)^{15}\text{O}$ reaction) leads to thermally unstable hydrogen burning. The temperature at the bottom of the hydrogen burning

⁴The literature is littered with multiple designations for these critical accretion rates that can lead to some confusion. We are following the notation of the recent review article by Lewin et al. (1995). Just for the sake of clarity, note that our \dot{M}_{c1} is the same as $\dot{M}_{st}(A)$ of Fujimoto et al. (1981) and \dot{M}_{c2} is the same as $\dot{M}_{st}(B)$. For some reason 1 and 2 are swapped in the article by Taam (1981).

shell (where $\epsilon_h y = X E_h \dot{m}$) is $T^4 = 3\kappa\epsilon_h y^2/2ac$, so that $T(H\ Shell) \approx 7 \times 10^8 \text{ K} (\kappa X^2 \dot{m}_5 / Z_{CNO})^{1/4}$. For stable hydrogen burning, we must have $T(H\ Shell) > 8 \times 10^7 \text{ K}$ or $\dot{m} > \dot{m}_{c2}$ where

$$\dot{m}_{c2} \approx \frac{6.3 \times 10^2 \text{ g cm}^{-2} \text{ s}^{-1}}{X} \left(\frac{0.04 \text{ cm}^2 \text{ g}^{-1}}{\kappa} \right)^{1/2} \left(\frac{Z_{CNO}}{0.01} \right)^{1/2}. \quad (36)$$

For accretion rates $\dot{m} < \dot{m}_{c2}$ the hydrogen ignition is unstable and initiates a flash. Our formula for \dot{m}_{c2} reproduces the quoted numbers in Fujimoto et al. (1981), Taam (1981) and Wallace et al. (1982) to within a factor of two for a large range in metallicities and neutron star masses and radii. This is reasonably good given the level of our approximations.

The ratio of these two critical accretion rates, $\dot{m}_{c1}/\dot{m}_{c2} \approx 5$ for a particular neutron star, pointing out that the unstable ignition in a pure helium layer occurs only for a limited range of accretion rates. These three critical accretion rates that delineate at least four different states of time dependent burning are summarized in Table 1. Just for the ease of comparing to other results, the global rates for a $1.4M_\odot$, $R = 10 \text{ km}$ neutron star accreting matter with $Z_{CNO} = 10^{-2}$ and $X = 0.7$ are also displayed. FHM also outlined the three time dependent cases, calling them cases 1-3, which are also noted in Table 1.

TABLE 1. Nuclear Burning Regimes at High Accretion Rates

Range in Local Accretion Rate	Type of Nuclear Burning
$\dot{m} > \dot{m}_{st}$ $\dot{M} > 2.6 \times 10^{-8} M_\odot \text{ yr}^{-1}$	Stable hydrogen/helium burning in a mixed H/He environment [Equations (24) and (26)]
$\dot{m}_{st} > \dot{m} > \dot{m}_{c1}$ $2.6 \times 10^{-8} > \dot{M}/(M_\odot \text{ yr}^{-1}) > 10^{-9}$ (FHM Case 1)	Thermally unstable helium ignition in a mixed H/He environment [Equation (35)]
$\dot{m}_{c1} > \dot{m} > \dot{m}_{c2}$ $10^{-9} > \dot{M}/(M_\odot \text{ yr}^{-1}) > 2 \times 10^{-10}$ (FHM Case 2)	Thermally unstable pure He ignition after complete hydrogen burning [Equation (36)]
$\dot{m}_{c2} > \dot{m}$ $2 \times 10^{-10} M_\odot \text{ yr}^{-1} > \dot{M}$ (FHM Case 3)	Thermally unstable hydrogen burning triggers combined flash

3.3. HELIUM IGNITION AT HIGH ACCRETION RATES

We initially assumed that the heat flux coming through the envelope prior to ignition was just that generated from the hot CNO cycle, or a value $F_{CNO} \approx \epsilon_h y_{ign}$ just prior to ignition. The typical ignition column density found in equation (34) was then independent of the local accretion rate and solely a function of the metallicity and neutron star parameters. This approximation breaks down at high accretion rates or low metallicities (possibly due to the spallation scenario of Bildsten et al. 1992) where other sources of energy release from the accumulating matter become important. It is easiest to see what happens by writing a flux (actually a combination of gravitational energy release and deeper burning) $F_{deep} = E_{deep} \dot{m}$ and ask what E_{deep} needs to be so as to compete with the flux in the envelope from the hot CNO cycle. This immediately tells us that if $E_{deep} \gtrsim (2 \times 10^{17} \text{ ergs g}^{-1} / \dot{m}_5) (Z_{CNO}/0.01)^{13/18}$, or only 0.2 MeV per accreted nucleon, then we need to reconsider the thermal state of the accumulating matter. We now go into this physics in some detail, as many of the interesting results from *EXOSAT* and *RXTE* are for neutron stars in this regime.

Let's start by rederiving the ignition condition for $F \propto \dot{m}$. Presume that the flux flowing through the envelope prior to ignition is $F = E_{deep} \dot{m}$ and leave E_{deep} as a free parameter. Then combining the ignition condition (equation [29]) with the temperature profile for an atmosphere carrying a constant flux F gives

$$y_{ign}(\dot{m}) \approx \frac{1.8 \times 10^8 \text{ g cm}^{-2}}{g_{14}^{4/13}} \left(\frac{0.04 \text{ cm}^2 \text{ g}^{-1}}{\kappa} \right)^{7/13} \left(\frac{10^{18} \text{ ergs g}^{-1}}{E_{deep} \dot{m}_5} \right)^{5/13} \quad (37)$$

which we compare to the previous ignition column density (equation [34]) to find the condition on accretion rate, metallicity and E_{deep} that must be satisfied so that the ignition column depends on \dot{m} . This gives

$$E_{deep} \gtrsim \frac{10^{17} \text{ ergs g}^{-1}}{\dot{m}_5} \left(\frac{0.04 \text{ cm}^2 \text{ g}^{-1}}{\kappa} \right)^{0.39} \left(\frac{1}{g_{14}} \right)^{0.222} \left(\frac{Z_{CNO}}{0.01} \right)^{13/18}. \quad (38)$$

So when this condition is satisfied we should expect that the critical column density depends on the accretion rate in the way given in equation (37).

Now, just how big is E_{deep} ? Well, there are a few energy sources to consider. The simplest is the energy released as matter falls a few scale heights in the atmosphere (i. e. the heat lost due to the non-adiabatic gravitational compression of the matter). This is roughly $E_{deep} \approx 5k_B T / 2\mu m_p$ or $10^{17} \text{ ergs g}^{-1}$ at $T = 3 \times 10^8 \text{ K}$. For normal metallicities, this energy release would only be relevant at \dot{m} 's so high that the burning is already

stable. This energy release is critical at lower metallicities and Bildsten & Brown (1997) show this for a case of $Z_{CNO} = 10^{-4}$. Figure 1 shows a case for $Z_{CNO} = 10^{-3}$, where this energy release is included. A much larger energy source is the deeper burning of residual hydrogen left from a previous flash (Ayasli & Joss 1982, Wallace et. al. 1982, Taam et al. 1993). Taam et al. (1993, 1996) have noted that the residual hydrogen left from a previous flash cannot burn until electron capture densities are reached (this is presumably due to the slowness of proton captures on the high Z nuclei). In this limit a fraction X_r of the accreting hydrogen is burned at large depths, giving $E_{deep} = 7.7 \times 10^{18} \text{ ergs g}^{-1} X_r$. This energy release is so large that even just a few percent of unburned hydrogen can be important.

Let's compare our simple estimates to the recent calculations of successive thermal instabilities by Taam et al. (1996). Their neutron star had $M = 1.4M_{\odot}$, $R = 9.1 \text{ km}$ and $X = 0.7$. They followed the time dependent evolution for models ranging from 0.1 – 1.0 times the Eddington limit. None of the models went into steady-state burning, so for this case \dot{M}_{st} is clearly in excess of \dot{M}_{Edd} . All models were time dependent and had substantial residual hydrogen, ranging at the highest \dot{m} 's from $X_r = 0.08 - 0.21$. Our formula gives $y_{ign} \approx 10^8 \text{ g cm}^{-2}$ over this range. Their accumulated columns as inferred from the time between ignitions was nearly constant at $y \approx \dot{m}t_{rec} \approx 5 \times 10^7 \text{ g cm}^{-2}$, and so our estimate is not so bad.

The energy release from deeper regions leads to, on average, higher ignition temperatures (up to $T = (3 - 4) \times 10^8 \text{ K}$) and lower ignition pressures. This allows for the distinct possibility that during the accumulation prior to ignition, even the Hot CNO cycle is modified, as breakouts can occur at these temperatures via the $^{15}\text{O}(\alpha, \gamma)^{19}\text{Ne}$ and $^{19}\text{Ne}(p, \gamma)^{20}\text{Na}$ reactions (see Champagne & Wiescher 1992 for an overview). The lower ignition pressures also leads to lower peak temperatures during the bursts and typically less fuel burned in a particular burst (Taam et al. 1996).

4. Time Dependent Burning and Type I X-Ray Bursts

What really happens as time marches on and accretion continuously dumps matter onto the star? The simplest time-dependent behavior is a limit cycle. The star would accumulate fuel for a time $t_{rec} = y_{ign}/\dot{m}$ until the thermal instability is reached, at which point the temperature rapidly rises and all of the fuel is burned. The first time-dependent numerical calculations found this type of behavior, but did not follow recurrent cycles. All that was found was the first burst and the ignition conditions for that burst were comparable to what is derived here. Before discussing in some detail what was learned from *EXOSAT* observations of Type I X-Ray bursts, let's discuss a few of the numbers that can be reliably predicted from theory.

4.1. BURST ENERGIES, RECURRENCE TIMES AND DURATIONS

When in the highest accretion rate unstable regime (see Table 1), the ignition columns (see equations [34] and [37]) are in the range $(5 - 20) \times 10^7 \text{ g cm}^{-2}$, giving recurrence times of $t_{rec} \sim 10^3 \text{ s} / \dot{m}_5$ or a few hours between bursts for a neutron star accreting at $10^{-9} M_\odot \text{ yr}^{-1}$. The burst energy is $E_{burst} \approx 4\pi R^2 y_{ign} E_{nuc}$ if all of the fuel is burned, giving

$$E_{burst} \approx 5 \times 10^{39} \text{ ergs} \left(\frac{R}{10 \text{ km}} \right)^2 \left(\frac{y_{ign}}{10^8 \text{ g cm}^{-2}} \right) \left(\frac{E_{nuc}}{4 \times 10^{18} \text{ ergs g}^{-1}} \right). \quad (39)$$

The flux from the burst is close to the Eddington limit, so that the duration is about the time it takes to radiate the nuclear energy at the Eddington limit, $t_{burst} \approx E_{burst} / L_{Edd} \sim 10 - 20 \text{ s}$. These three numbers, the burst energy, recurrence time and duration, are all in agreement with the observations and are the ‘‘hallmarks’’ of our understanding that Type I X-Ray bursts arise from thermonuclear instabilities in the accreted matter.

Let’s briefly discuss what happens as the thermal instability develops into a full-scale burst. There are many papers describing the time dependent behavior of the burning (e.g. Taam & Picklum 1979, Ayasli & Joss 1982, Wallace et al. 1982, Taam et al. 1993, 1996) and the resulting thermonuclear reactions of the ‘‘rp process’’ which produce elements beyond iron (Wallace & Woosley 1981, Taam 1985, Van Wormer et al. 1994, Schatz et al. 1997). As emphasized by FHM, the pressure at the bottom of the accumulated pile is an important quantity for the evolution of the flash. This is because the flash occurs at fixed pressure, and eventually the matter becomes radiation dominated. For a typical ignition column of 10^8 g cm^{-2} , the pressure is $P = gy \approx 10^{22} \text{ ergs cm}^{-3}$, so $aT_{max}^4/3 \approx P$ gives a maximum temperature $T_{max} \approx 1.5 \times 10^9 \text{ K}$. At this temperature, the degeneracy is lifted and the thermal time (from equation [8]) at the bottom of the burning material is about one second. In one-dimensional (i.e. spherically symmetric) burning, convection nearly always occurs before these maximum temperatures are reached. However, this only acts to transport the heat upwards a few scale heights, as the convective zone never reaches the photosphere (Joss 1977). The energy is ultimately taken out of the star via radiative diffusion. The physical thickness of the burning layer is $H \approx 5k_B T / 2\mu m_p g \approx 18.5 \text{ m} T_9$, or about 20 meters thicker than before the thermal instability set in.

4.2. WHAT WAS LEARNED FROM *EXOSAT* OBSERVATIONS

The original information about Type I X-ray bursters came from low-Earth orbit satellites. These discovered the phenomena and the combination of theory and observation led to a firm belief that the bursts arose from ther-

monuclear instabilities (see Lewin et. al. 1995). However, the frequent data gaps and absence of long-term observations hindered studies of the accretion rate dependence of the phenomena.

The 3.8 day orbit of *EXOSAT* was an excellent match for long-term monitoring of bursters, thus revealing the dependence of their nuclear burning behavior on accretion rate. As noted above, in the simplest picture of a recurrent cycle, the time between bursts should decrease as \dot{M} increases since it takes less time to accumulate the critical amount of fuel. Exactly the *opposite* behavior was observed from many low accretion rate ($\dot{M} \sim 10^{-9} M_{\odot} \text{ yr}^{-1}$) neutron stars. A particularly good example is 4U 1705-44, where the recurrence time increased by a factor of ≈ 4 when the accretion rate increased by a factor of ≈ 2 (Langmeier et al. 1987, Gottwald et al. 1989). This is difficult to understand in terms of what we discussed in §3. If the star is accreting matter with $Z_{CNO} = 10^{-2}$ then these accretion rates are at the boundary ($\dot{M} \sim \dot{M}_{c1}$) of unstable helium ignition in a hydrogen-rich environment at high \dot{M} and unstable pure helium ignition at lower \dot{M} . The expected change in burst behavior as \dot{M} increases would then be to more energetic and more frequent bursts. This was not observed. The difficulties are still present if we reduce the metallicities via spallation.

Other low \dot{M} neutron stars showed similar behavior (see Bildsten's [1995] discussion of many of the "atoll" sources), each of which showed longer (and less periodic) recurrence times as \dot{M} increased. More importantly, the amount of fuel consumed in the bursts became much less than that accreted between bursts as \dot{M} increased. van Paradijs, Penninx & Lewin (1988) tabulated this effect for many X-ray burst sources and concluded that increasing amounts of accreting fuel are consumed in a less visible way than Type I X-ray bursts as \dot{M} increases. The objects they studied have all had Eddington limited radius expansion bursts and so the ratio of the persistent flux to the flux during radius expansion measured the accretion rate in units of Eddington accretion rate. From this, one infers that these objects typically accrete at rates $\dot{M} \approx (3-30) \times 10^{-10} M_{\odot} \text{ yr}^{-1}$.

There are six higher accretion rate "Z" sources (Sco X-1, Cyg X-2, GX 5-1, GX 17+2, GX 340+0, GX 349+2, Hasinger & van der Klis 1989), which are thought to be accreting near the Eddington limit of $10^{-8} M_{\odot} \text{ yr}^{-1}$ (Fortner, Lamb & Miller 1989, Miller & Lamb 1992). Their nuclear burning might be stable some of the time, as they vary in accretion rate by a factor of 2 - 3. None of these are known to exhibit periodic bursting behavior, and only two (Cygnus X-2 and GX 17+2) have ever shown Type I X-ray bursts. The first burst found was from Cygnus X-2 (Kahn & Grindlay 1984). It had a rise time < 2.56 s and a decay time $\approx 5 - 10$ s, but little else was certain from this observation. Kuulkers, van der Klis & van Paradijs (1995) found nine events from Cygnus X-2 which are reasonably

interpreted as Type I X-ray bursts. They all lasted about 3 seconds, had peak fluxes less than the persistent flux, and burst energies $\sim 10^{38}$ ergs. However, they were so infrequent that the resulting α value was usually $> 10^3$ and sometimes $> 10^4$. In other words, these bursts were not burning all of the accreted fuel. RXTE has seen one type I X-ray burst from Cygnus X-2 (Smale 1997). Many bursts have been observed from GX 17+2 (Tawara et al. 1984, Sztajno et al. 1986, Kuulkers et al. 1997) all of which have $\alpha \gtrsim 10^3$ and long durations (typically 100 seconds) implying that little of the accreted fuel is consumed in the bursts.

5. Beyond One-Dimensional Theories

If Type I X-ray bursts are the only manifestation of unstable burning, then frequent energetic bursts should be seen from all weakly magnetic and sub-Eddington neutron stars. *EXOSAT* did not find see this occur, nor have other satellites. One solution to this mystery is to assume that the accumulating matter only covers 10 % of the stellar area (say in the equatorial region if the matter is fed in via a thin accretion disk), thus increasing the local accretion rate. This might help with the Atoll sources, as the burning would become stable when the global rate exceeds $\dot{M} \approx 10^{-9} M_{\odot} \text{yr}^{-1}$. However, it implies that the fuel stays in the equatorial region until it reaches ignition pressures. It is not clear that this is possible, especially since the accumulated matter is substantially lighter than the ashes from burning. This solution would not work for the Z sources, as they have shown bursts (though infrequent) and would be absolutely stable if the local accretion rate was a factor of 10 larger. One could appeal to the spherical flows and magnetic funneling implied by some for the QPO phenomenology (Alpar & Shaham 1985, Miller & Lamb 1992) to have factors of two enhancement in the local accretion rate. This would allow some Z source to be stable and others not.

Rather than invoking alternative accretion scenarios to explain the burst phenomenology, let's presume that the accumulated matter covers most of the star before it undergoes a thermonuclear instability and see if there is some physics we have previously omitted that now needs to be considered. The most likely candidate is the propagation of burning fronts around the star.

5.1. IGNITION AND PROPAGATION OF BURNING IN BURSTS

Once it was understood that the X-ray bursts were thermonuclear flashes, a few workers in the field (Joss 1978, Ruderman 1981, Shara 1982, Livio & Bath 1982) pondered the possibility that the burning was not spherically symmetric. In this case, there would be an ignition site somewhere on the

star (most likely where \dot{m} is highest) that would start a nuclear “fire” which spreads around the star by igniting the accumulated fuel. The bursts rise to a peak luminosity in about one second and are known (from the spectral evolution and energetics) to cover the whole star, thus requiring a lateral propagation speed of at least 10^6 cm s⁻¹. The fundamental reason to seriously consider this scenario is that it takes many hours to accumulate a thermally unstable pile of fuel, but only 10 seconds to burn it. Thus, the conditions must be identical to better than a part in 1000 for the local thermal instability to occur simultaneously over the whole star. This seems difficult to arrange in the accretion environment.

One of the best quotes about what might be gained by relaxing the spherically symmetric assumption was from Joss (1978):

“Our computations do not reproduce the complex and individualized burst structure and recurrence patterns that have been observed in some burst sources. It is possible that many of these complexities result from violations of spherical symmetry due to stellar rotation or non-spherical accretion. Such effects could allow a limited portion of the neutron star surface to undergo a flash that then ignites other regions, in a manner that varies from burst to burst and from one source to another.”

Following this, a few (Fryxell & Woosley 1982, Nozakura, Ikeuchi & Fujimoto 1984, Bildsten 1993, 1995) have estimated the lateral propagation speeds for burning fronts on neutron stars. The heating of the gas from the thermal instability occurs on a timescale of seconds, which is $10^5 - 10^6$ times longer than the time it takes for sound to cross a scale height. The atmosphere has plenty of time to hydrostatically adjust to the changing temperature, thus making detonations very unlikely. So, let’s begin by estimating the lateral deflagration speed.

The cold fuel ahead of the moving burning front is ignited by diffusive heating from the ashes. A steady burning front thus has a characteristic thickness, which is the distance where diffusive heating is comparable to the nuclear heating $l \approx (acT_f^4/3\kappa\rho^2\epsilon_{3\alpha})^{1/2}$, where T_f is the undetermined burning temperature. The front propagates through l in the time it takes the nuclear burning to heat the gas to T_f , $t_{nuc} \approx C_p T_f / \epsilon_{3\alpha}$, giving a speed

$$v \sim \frac{l}{t_{nuc}} \sim \left(\frac{acT_f^2\epsilon_{3\alpha}}{3C_p^2\rho^2\kappa} \right)^{1/2} \sim \frac{h}{(t_{th}t_{nuc})^{1/2}}. \quad (40)$$

This estimate is sensitive to the value T_f , thus requiring a more careful derivation than provided by (40). However, it is a good initial guess and gives (for $P \approx 10^{22}$ erg cm⁻³) values of order 100 – 1000 cm s⁻¹. Higher ignition pressures can increase this by a factor of ~ 10 , but it seems difficult (if not impossible) to reach the 10^6 cm s⁻¹ needed for bursts.

Though the exact value of the deflagration speed is uncertain, there is an accurate lower bound that comes from considering the quenching of a burning front. Propagation is halted when the lateral thickness of the front, l , exceeds a pressure scale height, $h = P/\rho g$. In this case most of the released nuclear energy is radiated to vacuum rather than used to heat adjacent unburned matter. Since $l \sim h(t_{nuc}/t_{th})^{1/2}$, propagation requires enough fuel so that $t_{nuc} \lesssim t_{th}$ at the burning temperature, translating into a minimum column density (or pressure) for successful propagation (a “flammability” limit, which for pure helium accretion is $y_{min} \approx 10^8 \text{ g cm}^{-2}$) and a minimum speed $v_{min} \sim h/t_{th} \sim 100 \text{ cm s}^{-1}$ (Bildsten 1995).⁵

The propagation speed is most likely much larger when convection is occurring (Fryxell & Woosley 1982). The enhanced mixing and lateral motions will increase the propagation speeds over the laminar values. The convection is very efficient at transporting heat, as the time for sound to cross a scale height $t_c \sim c_s/g \sim 10^{-6} \text{ s}$ is much shorter than the local thermal time. Steady-state convection then brings the temperature-density profile in the envelope very close to the adiabatic value, regardless of the choice of a mixing length. Crude dimensional analysis with a mixing length, l_m gives a convective velocity

$$v_c \sim c_s \left(\frac{l_m}{h} \right)^{1/3} \left(\frac{c_s/g}{t_{th}} \right)^{1/3} \sim 10^6 \text{ cm s}^{-1}, \quad (41)$$

a value comparable to what is needed for the rise time of a Type I X-ray burst. The fact that the turbulent scale is close to a scale height prohibits us from doing much more than saying that the propagation speed is comparable to the convective velocity when convection occurs.

5.2. LATERAL PROPAGATION AND OBSERVATIONS

Now, how do we expect the propagation speeds to affect the observations? In the presence of convection, the high combustion speed ($v \gtrsim 10^6 \text{ cm s}^{-1}$) leads to rapid ignition ($\lesssim 10 \text{ s}$) of all connected parts of the surface which have enough fuel for convective combustion. This is the dominant burning mode at low \dot{M} 's, where the column densities prior to ignition are large. Most of the star is then convectively combustible at any one time, so that a recurrent thermal instability leads to quasi-periodic Type I X-ray bursting.

However, as \dot{M} increases (especially in the range above $10^{-9} M_\odot \text{ yr}^{-1}$) the ignition columns are decreasing (see §3.3 and Taam et al. 1996) and

⁵There is a possibility that the ignition columns become so low at high \dot{M} 's that the burning fronts are completely quenched, in which case no lateral propagation can occur. The resulting time dependent burning in this limit would be very difficult to observe, as the number of independent patches on the star would be very large. This has yet to be calculated for the mixed hydrogen/helium burning.

convection becomes less prevalent. In this regime, the slower burning speeds are more prevalent. This breaks the burst periodicity, reduces the amount of fuel available for Type I X-ray bursts, and leads to slow burning of the accumulated matter on the neutron star. In this regime, the combustion front moves at a speed $\sim 1000 \text{ cm s}^{-1}$, so that a “ring of fire” of horizontal width $vt_{th} \sim 100$ meters moves out from the local instability. Most importantly, the time for the fire to go around the star ($R/v \sim 10^3\text{s}$) is comparable to the fuel accumulation time so that only a few fires are burning at once (Bildsten 1995). A single fire gives a luminosity profile that roughly looks like

$$L_{fire}(t) \approx F(2\pi vt)(vt_{th}) \approx E_{nuc} y_{ign} 2\pi v^2 t, \quad (42)$$

where F is the local flux. When only a few fires are burning at one time, the nuclear burning luminosity appears as \sim hour-long flares of amplitude $L_n \approx E_{nuc} \dot{M}$, or 1 – 5 % of the accretion luminosity (Bildsten 1995).

5.3. DOES UNSTABLE NUCLEAR BURNING CAUSE THE VERY LOW FREQUENCY NOISE?

Hasinger & van der Klis’s (1989) analysis of *EXOSAT* observations of the brightest LMXBs characterized the time dependence of the X-ray flux from many neutron stars. They found that excess power in the mHz-Hz range was often present and sometimes correlated with other source properties. This noise has a spectral density between flicker noise ($\propto 1/f$) and even steeper ($\propto 1/f^2$) noise and was dubbed the “very low frequency noise” (VLFN) by van der Klis et al. (1987). In the time domain, it looks like $\sim 1 - 5\%$ luminosity variations on minute to hour long time-scales, comparable to what we just described might be produced at high accretion rates from the slow burning fires.

The best way to decide if the VLFN has anything to do with nuclear burning is to see if the strength of the hour-long flares (i.e. the VLFN) correlates with the Type I X-ray bursts. One would not expect a correlation if the VLFN was from accretion fluctuations. Bildsten (1995) collated the *EXOSAT* X-ray burst data with the measured VLFN power and found a continuum of behavior in the brightest accreting X-ray sources. On one end of the continuum are the sources that always show strong VLFN and never show enough Type I X-ray bursts to burn all of the fuel (the Z sources), while on the other end are those objects which are always bursting and never show VLFN (the lowest accretion rate Atoll sources). The most illuminating objects are three (4U 1705-44, 4U 1636-53 and 4U 1735-44) which show X-ray bursts and VLFN simultaneously. The varying \dot{M} ’s for these objects allows them to display a continuum of behavior. The VLFN is absent, or much reduced, when the neutron star is undergoing regular Type I X-ray

bursts, and increases in strength as the bursts become less fuel-consuming and aperiodic at higher \dot{M} 's.

The correlation found by Bildsten (1995) points to the concept that as the accretion rate increases, there is a tradeoff of nuclear fuel between X-ray bursts and VLFN, favoring VLFN at high accretion rates. It also implies that the burning should be asymmetric on the star, allowing for measurements of the spin period. We discuss this in §7.

6. The Role of a Magnetic Field

A Type I X-ray burst has never been seen from a magnetized ($B \gtrsim 10^{12}$ G) accreting pulsar. This has led to the oft-quoted quip that “X-Ray pulsars don’t burst”. The lack of bursts from accreting pulsars was surprising since they accrete at rates comparable to the X-ray bursters. Joss & Li (1980) first explained the lack of bursts by *stabilizing* the nuclear burning with a high local accretion rate ($\dot{m} > \dot{m}_{st}$).⁶ The magnetic field funnels the accretion onto the polar cap and confines the accreted matter all the way to the ignition pressure. The constraint of $\dot{m} > \dot{m}_{st}$ is easily satisfied for pulsars with $\dot{M} \gtrsim 10^{-10} M_{\odot} \text{ yr}^{-1}$, as the fractional area of the polar cap only needs to satisfy $A_{\text{cap}}/4\pi R^2 \lesssim 0.01$. This is well within the estimates obtained by either following the field lines from the magnetospheric radius to the star (Lamb, Pethick, & Pines 1973), or allowing the matter to penetrate through the magnetopause via a Rayleigh-Taylor instability and attach to field lines at smaller radii (Arons & Lea 1976; Elsner & Lamb 1977).

However, given the range in magnetic field strengths and accretion rates, it seems unlikely that this could explain the absence of Type I X-ray bursts in *all* accreting pulsars. Bildsten (1995) thus suggested that, even when the burning is thermally unstable, a strong magnetic field might inhibit the rapid lateral convective motion needed for the combustion front to rapidly ignite the whole star (or polar cap). The burning front would then propagate at the slower speed set by diffusive heat transport. In this case, the nuclear burning would appear as a flare with a duration of a few minutes to an hour (depending on the propagation speed and the lateral extent of the fuel-rich region). These flares would rise on a timescale comparable to the duration and not necessarily be asymmetrical in time.

The field strength required to halt the convective ($\sim 10^6 \text{ cm s}^{-1}$) propagation of burning fronts is not known. Convection is potentially stabilized when $B^2 > 8\pi P_{\text{ign}}$ (Gough & Tayler 1966), which requires $B \gtrsim 7 \times 10^{11}$ G

⁶Joss & Li (1980) also suggested that the reduction of the opacity in an ultra-strong ($B > 10^{13}$ G) field could stabilize burning for $\dot{m} < \dot{m}_{st}$. This is at odds with the recent abstract by Lamb, Miller and Taam (1996), who suggested that the reduced opacity would increase the critical accretion rate above which the burning becomes stable. Our equation (24) gave $\dot{m}_{st} \propto \kappa^{-3/4}$, and we agree with Lamb et al.’s suggestion.

in the helium burning regions. This is satisfied for most accreting pulsars. However, there are subtleties even at weaker magnetic fields, as the convection occurs in a region with $\rho \approx 8 \times 10^5 \text{ g cm}^{-3}$, giving a local ram pressure when in steady-state convection of $P_{ram} \approx \rho v_c^2 \ll P$. This can most likely push around a magnetic field with strength $B \lesssim (8\pi\rho v_c^2)^{1/2} \approx 5 \times 10^9 \text{ G}$, but we do not really know how convection (and most importantly burning front propagation) is altered by magnetic fields in the interesting intermediate range $\rho v_c^2 \ll B^2/8\pi \ll P$ ($5 \times 10^9 \text{ G} < B < 7 \times 10^{11} \text{ G}$).

We emphasize that the appearance of the instability (i.e., whether it looks like a Type I X-ray burst or a flare lasting a few minutes) will yield crucial information on the neutron star’s surface magnetic field. The accreting pulsars most likely to yield time-dependent burning phenomena are either ones with low fields (like GRO J1744-28, Bildsten & Brown 1997) or very low accretion rates. Strohmayer et al. (1997) searched for Type I X-ray bursts from GRO J1744-28, but could not find any. The Type I X-ray bursts that they did detect were from another source. Perhaps the best objects to survey would be the faint and weakly magnetic “6-second pulsars” (1E 2259+586, 1E 1048.1-5937 and 4U 0142+61, see Mereghetti & Stella 1995). The inferred fields from their steady spin down are $\lesssim 10^{12} \text{ G}$ and the global accretion rates are $\lesssim 10^{-11} M_\odot \text{ yr}^{-1}$. These objects could very well be unstably burning. The burst (or flare) recurrence time and energetics completely depends on whether the matter stays confined to the polar cap prior to ignition. Magnetohydrostatic calculations (Hameury et. al. 1983, Brown & Bildsten 1997) suggest that the matter does stay confined on the cap, in which case the recurrence time will be shorter than expected for spherical accretion and the burst energetics much smaller. Actually, the burst energy would just be $E_{burst} \approx A_{cap} E_{nuc} y_{ign}$, a value much smaller (potentially two to three orders of magnitude) than the typical Type I X-ray burst. Gotthelf & Kulkarni (1997) might have just detected such an event from an unknown (and very faint, $L_Q < 10^{33} \text{ ergs s}^{-1}$) object in the globular cluster M28. They found a very subluminescent Type I X-ray burst with $L \sim 4 \times 10^{36} \text{ ergs s}^{-1}$ and total burst energy of $2 - 3 \times 10^{37} \text{ ergs}$, consistent with complete burning over a small fraction of the star.

7. Observed Periodicities During Type I X-Ray Bursts

There were many early (but statistically weak) indications of periodicities during Type I X-ray bursts that led Livio & Bath (1982) to speculate upon the possibilities of rotation or surface waves as the source of periodicity. McDermott & Taam (1987) calculated the g-mode frequencies of the envelope during a type I X-ray burst and showed that the modes would rapidly change their frequency (by a factor of 2 in 10 seconds). The first convincing

case of a highly coherent oscillation during a Type I X-ray burst was that found by Schoelkopf & Kelley (1991) in Aql X-1 at 7.6 Hz. They argued that the periodicity was the neutron star rotation period and that the signal arose when the burning asymmetries were rotated in and out of view.

Jongert & van der Klis (1996) searched for pulsations from 147 Type I X-Ray bursts detected by EXOSAT. Nothing was found, with typical fractional RMS amplitude limits of 2-6 % for frequencies up to (typically) 256 Hz. The recent launch of the *Rossi X-Ray Timing Explorer* (RXTE) has dramatically changed this situation. Even though it is likely that our discussion of these results will be dated by the time this article appears, it is important to summarize what has been found so far. Table 2 contains a summary of what was known as of May 1997.

TABLE 2. Rapid Periodicities During Type I X-Ray Bursts (as of May 1997)

Object Name	ν_B (Hz)	ν_d (Hz)	Reference
4U 1728-34	363	363	Strohmayer et. al. 1996
KS 1731-260	524	260 ± 10	Smith et al. 1997, Wijnands & van der Klis
Aql X-1	7.6,549	–	Schoelkopf & Kelley 1991, Zhang et al. 1997b
4U 1636-53	581	276 ± 10	Zhang et al. 1997a, Wijnands et al. 1997
MXB 1743-29	589	–	Strohmayer et al. 1997

Strohmayer et al. (1996) found nearly coherent $\nu_B = 363$ Hz oscillations during type I X-ray bursts from the atoll source 4U 1728-34. Pulsations with amplitudes of 2.5 – 10% were detected in six of the eight bursts analyzed at that time. In addition, two separate high frequency QPO’s were found in the persistent emission. These changed with accretion rate, but maintained a fixed difference frequency of $\nu_d = 363$ Hz, identical to the period seen during the bursts. They suggested a “beat” frequency-like model and associated the 363 Hz feature with the neutron star spin.

Smith, Morgan & Bradt (1997) found a $\nu_B = 523.92 \pm 0.05$ Hz oscillation during the peak of a single Type I X-ray burst from KS 1731-260. This burst had radius expansion and the periodicity was only found at the end of the contraction phase. The oscillation was very coherent ($Q > 900$) and had a pulse fraction of 6%. No harmonics were detected. Wijnands & van der Klis (1997) found kHz QPO’s from this object at a fixed difference frequency $\nu_d = 260 \pm 10$ Hz, consistent with one-half the frequency seen during the bursts. Another object, 4U 1636-53, has a difference frequency in the kHz QPO’s of $\nu_d = 276 \pm 10$ Hz (Wijnands et al. 1997) and a burst frequency of $\nu_B = 581$ Hz (Zhang et al. 1997a), not quite consistent with twice the

difference frequency. Strohmayer et al. detected 589 Hz oscillations during three Type I X-ray bursts from an object (most likely MXB 1743-29) near the galactic center. These bursts were temporally separated by just over a month and the oscillations were detected in the few seconds after the burst peak.

The frequency during the bursts from both MXB 1743-29 and 4U 1728-34 increased by a few Hz as the neutron star atmosphere cools. There is no torque large enough to change the neutron star spin this rapidly, so Strohmayer et al. (1997) have argued that the observed periodicity is the rotation rate of the burning shell. They noted that the slight ($\Delta r \ll R$) hydrostatic expansion during the burning can explain the observations if the shell conserves angular momentum. In that case, the change in thickness (estimated from §'s 3.1 and 4.1 to be $\Delta r \approx 20$ meters) will lead to a frequency change of the burning material by an amount $\Delta\nu \approx \nu(\Delta r/R) \approx 2 \times 10^{-3}\nu$, or a change of 1 Hz for a 500 Hz rotation. This is close to what is observed. It is presumed that the neutron star spin frequency is the higher value and is, of course, unchanging throughout the burst.

However, the observed frequency evolution is always from low to high during the cooling phase of the burst. Why is this? It is most likely because the atmospheric scale height is decreasing during the cooling phase. The atmosphere expanded and spun-down at the onset of the thermonuclear instability. However, this spin-down is difficult to observe, as the radiative layer (see discussion in §4.1) delays the information about the burst, so that by the time the observer sees it, the expansion and spin-down has already occurred. There might be some bursts where the spin-down evolution can be detected. Such a detection would obviously make us much more confident of Strohmayer et al's (1997) interpretation.

Their conjecture implies that the burning matter wraps around the star a few times during the instability, as the relative shear is a few Hz for many seconds. Shear layers are typically unstable to the Kelvin-Helmholtz instability. However, the buoyancy due to the mean molecular weight contrast or even thermal (i.e. the buoyancy in equation [12]) can easily stabilize this shear (at least for a dynamical time) as the Richardson number $Ri = N^2/(dv_{rot}/dz)^2 \gg 1/4$ (Fujimoto 1988). The shear might thus persist for the few seconds required. Further theoretical studies need to be carried out to fully understand the repercussions of this result. Problems that immediately come to mind are the role of any magnetic field and more importantly, the possibility of longer timescale rotational instabilities (such as the baroclinic instability). Basically, one must rule out any mechanism that can transport angular momentum to the shell in less than ten seconds. That is a very long time on the neutron star, about 10^7 sound crossing times!

8. Acknowledgements

I would like to thank the organizers of this Advanced Study Institute for carrying out a flawless meeting and Jan van Paradijs for his patience with my late submission. This article has greatly benefited from countless conversations with Ed Brown about the subtleties of nuclear burning and settling on accreting neutron stars. Andrew Cumming simulated the signals expected from propagating combustion fronts on rotating neutron stars and helped me think through the theoretical repercussions of the recent RXTE results. Tod Strohmayer was kind enough to show me a large amount of RXTE data on periodicities during Type I X-ray bursts and Bob Rutledge provided early insights into the phenomenology of periodicities during the bursts. This research was supported by NASA via grants NAG 5-2819 and NAGW-4517 and by the Alfred P. Sloan Foundation.

References

- Alpar, M. A. & Shaham, J. 1985, *Nature*, 316, 239
 Arons, J., & Lea, S. M. 1976, *Ap. J.*, 207, 914
 Ayasli, S., & Joss, P. C. 1982, *Ap. J.*, 256, 637
 Belian, R. D., Conner, J. P., & Evans, W. D. 1976, *Ap. J.*, 206, L135
 Bildsten, L. 1993, *Ap. J.*, 418, L21
 Bildsten, L. 1995, *Ap. J.*, 438, 852
 Bildsten, L. & Brown, E. F. 1997, *Ap. J.*, 477, 897
 Bildsten, L. & Cutler, C. 1995, *Ap. J.*, 449, 800
 Bildsten, L., Salpeter, E. E., & Wasserman, I. 1992, *Ap. J.*, 384, 143
 Bildsten, L., Salpeter, E. E., & Wasserman, I. 1993, *Ap. J.*, 408, 615
 Brown, E. F. & Bildsten, L. 1997, submitted to *Ap. J.*
 Caughlan, G. R. & Fowler, W. A. 1988, *Atomic Data Nucl. Data Tables*, 40, 283
 Champagne, A. E. & Wiescher, M. 1992, *Ann. Rev. Nucl. Part. Sci.*, 42, 39
 Cox, J. P. 1980, *Theory of Stellar Pulsation* (Princeton: Princeton Univ. Press)
 Elsner, R. F., & Lamb, F. K. 1977, *Ap. J.*, 215, 897
 Finger, M. H., Koh, D. T., Nelson, R. W., Prince, T. A., Vaughan, B. A. & Wilson, R. B. 1996, *Nature*, 381, 291
 Fortner, B., Lamb, F. K. & Miller, G. S. 1989, *Nature*, 342, 775
 Fryxell, B. A., & Woosley, S. E. 1982, *Ap. J.*, 261, 332
 Fujimoto, M. Y., Hanawa, T., & Miyaji, S. 1981, *Ap. J.*, 247, 267 (FHM)
 Fujimoto, M. Y., Sztajno, M., Lewin, W. H. G., & van Paradijs, J. 1987, *Ap. J.*, 319, 902
 Fujimoto, M. Y. 1988, *A&A*, 198, 163
 Fushiki, I., & Lamb, D. Q. 1987, *Ap. J.*, 323, L55
 Gotthelf, E. V. & Kulkarni, S. R. 1997, in preparation
 Gottwald, M. et al. 1989, *Ap. J.*, 339, 1044
 Gough, D. O., & Tayler, R. J. 1966, *MNRAS*, **133**, 85
 Grindlay, J. et al. 1976, *Ap. J.*, 205, L127
 Hameury, J. M., Bonazzola, S., Heyvaerts, J. & Lasota, J. P. 1983, *A&A*, 128, 369
 Hanawa, T. & Fujimoto, M. Y. 1982, *PASJ*, 34, 495
 Hansen, C. J. & Kawaler, S. D. 1994, *Stellar Interiors: Physical Principles, Structure and Evolution* (New York: Springer Verlag)
 Hansen, C. J. & Van Horn, H. M. 1975, *Ap. J.*, 195, 735
 Hasinger, G. & van der Klis, M. 1989, *A&A*, 225, 79

- Hoyle, R. & Fowler, W. A. 1965 in *Quasi-Stellar Sources and Gravitational Collapse*, ed. I. Robinson, A. Schild, and E. L. Schucking (Chicago: University of Chicago Press)
- Jongert, H. C. & van der Klis, M. 1996, *A&A*, 310, 474
- Joss, P. C. 1977, *Nature*, 270, 310
- Joss, P. C. 1978, *Ap. J.*, 225, L123
- Joss, P. C., & Li, F. K. 1980, *Ap. J.*, 238, 287
- Kahn, S. M. & Grindlay, J. E. 1984, *Ap. J.*, 281, 826
- Kouveliotou, C. et al. 1996, *Nature*, 379, 799
- Kuulkers, E., van der Klis, M. & van Paradijs, J. 1995, *Ap. J.*, 450, 748
- Kuulkers, E., van der Klis, M., Oosterbroek, T., van Paradijs, J. & Lewin, W. H. G. 1997, to appear in *MNRAS*.
- Lamb, D. Q., & Lamb, F. K. 1978, *Ap. J.*, 220, 291
- Lamb, D. Q., Miller, M. C. & Taam, R. E. 1996, *BAAS*, 188, 84.02
- Lamb, F. K., Pethick, C. J. & Pines, D. 1973, *Ap. J.*, 184, 271
- Langmeier, A., Sztajno, M., Hasinger, G., Trümper, J., & Gottwald, M. 1987, *Ap. J.*, 323, 288
- Lewin, W. H. G., van Paradijs, J., & Taam, R. E. 1995, in "X-Ray Binaries", ed. W. H. G. Lewin, J. van Paradijs & E. P. J. van den Heuvel (London: Cambridge), p. 175
- Livio, M. & Bath, G. T. 1982, *A&A*, 116, 286
- Maraschi, L. & Cavaliere, A. 1977, *Highlights Astron.*, 4, 127
- McDermott, P. N. & Taam, R. E. 1987, *Ap. J.*, 318, 278
- Mereghetti, S. & Stella, L. 1995, *Ap. J.*, 442, L17
- Miller, G. S. & Lamb, F. K. 1992, *Ap. J.*, 388, 541
- Nelson, L. A., Rappaport, S. & Joss, P. C. 1986, *Ap. J.*, 304, 231
- Nozakura, T., Ikeuchi, S. & Fujimoto, M. Y. 1984, *Ap. J.*, 286, 221
- Ruderman, M. 1981, *Prog. Part. and Nucl. Phys.*, 6, 215
- Schoelkopf, R. J. & Kelley, R. L. 1991, *Ap. J.*, 375, 696
- Schatz, H. et al. 1997, to appear in *Physics Reports*
- Schwarzschild, M. 1958, *Structure and Evolution of the Stars* (New York: Dover Publications)
- Schwarzschild, M. & Härm, R. 1965, *Ap. J.*, 142, 855
- Shara, M. M. 1982, *Ap. J.*, 261, 649
- Shore, S. N., Livio, M. & van den Heuvel, E. P. J. 1994, *Interacting Binaries* (New York: Springer)
- Smale, A. P. 1997, private communication
- Smith, D. A., Morgan, E. H. & Bradt, H. 1997, *Ap. J.*, 479, L137
- Strohmayer, T. E., Zhang, W., Swank, J. H., Smale, A., Titarchuk, L., Day, C. & Lee, U. 1996, *Ap. J.*, 469, L9
- Strohmayer, T. E., Jahoda, K., Giles, B., & Lee, U. 1997, *Ap. J.*, to appear.
- Sztajno, M., van Paradijs, J., Lewin, W. H. G., Langmeier, A., Trümper, J., & Pietsch, W., 1986, *MNRAS*, 222, 499
- Taam, R. E. 1980, *Ap. J.*, 241, 358
- Taam, R. E. 1981, *Astrop. & Space Science*, 77, 257
- Taam, R. E. 1982, *Ap. J.*, 258, 761
- Taam, R. E. 1985, *Ann. Rev. Nuc. Part. Sci.*, 35, 1
- Taam, R. E., & Picklum, R. E. 1978, *Ap. J.*, 224, 210
- Taam, R. E., & Picklum, R. E. 1979, *Ap. J.*, 233, 327
- Taam, R. E., Woosley, S. E., Weaver, T. A., & Lamb, D. Q. 1993, *Ap. J.*, 413, 324
- Taam, R. E., Woosley, S. E., & Lamb, D. Q. 1996, *Ap. J.*, 459, 271
- Tawara, Y., Hirano, T., Kii, T., Matsuoka, M. & Muakami, T. 1984, *PASJ*, 36, 861
- van der Klis, M. et al. 1987, *Ap. J.*, 313, L19
- van Paradijs, J., Penninx, W. & Lewin, W. H. G. 1988, *MNRAS*, 233, 437
- Van Wormer, L., Görres, J., Iliadis, C., Wiescher, M., & Thielemann, F.-K. 1994, *Ap. J.*, 432, 326
- Wallace, R. K., & Woosley, S. E. 1981, *Ap. J. Suppl.*, 43, 389

- Wallace, R. K., Woosley, S. E. & Weaver, T. A. 1982, *Ap. J.*, 258, 696
- Wijnands, R. A. D., van der Klis, M., van Paradijs, J., Lewin, W. H. G., Lamb, F. K.,
Vaughan, B. & Kuulkers, E. 1997, *Ap. J.*, 479, L141
- Wijnands, R. A. D. & van der Klis, M., 1997, to appear in *Ap. J. Letters*.
- Woosley, S. E. & Taam, R. E. 1976, *Nature*, 263, 101
- Zhang, W., Lapidus, I., Swank, J. H., White, N. E., & Titarchuk, L. 1997a, *IAUC*, 6541
- Zhang, W., et al. 1997b, to be submitted to *Ap J Letters*